BMC Genomics

RESEARCH ARTICLE **Open Access**

Insights on bio-degumming of kenaf bast based on metagenomic and proteomics

Sheng Wen Duan, Li Feng Cheng, Xiang Yuan Feng, Qi Yang, Zhi Yuan Liu, Ke Zheng and Yuan De Peng[*]

Abstract

Background: Microbes play important roles in kanef-degumming. This study aims at identifying the key candidate microbes and proteins responsible for the degumming of kenaf bast (*Hibiscus cannabinus*). Kenaf bast was cut into pieces and immersed into microbia fermentation liquid collected from different sites. Fermentation liquid samples were collected at 0, 40, 110 and 150 h and then subjected to the 16S/18S rRNA sequencing analysis and isobaric tag for relative and absolute quantitation (iTRAQ) analysis. The microbial (bacterial and fungal) diversity and the differentially expressed proteins/peptides (DEPs) were identified.

Results: With the prolonged degumming time, the weight loss rate increased, the bacterial diversity was decreased. [Weeksellaceae], *Enterobacteriaceae* and *Moraxellaceae* were rapidly increased at 0~40 h, and then decreased and were gradually replaced by *Bacteroidaceae* from 40 h to 150 h. Similarly, *Chryseobacterium* and *Dysgonomonas* were gradually increased at 0~110 h and then decreased; *Acinetobacter* and *Lactococcus* were increased at 0~40 h, followed by decrease. *Bacteroides* was the dominant genus at 150 h. Sequencing 18S rRNA-seq showed the gradually decreased *Wallemia hederae* and increased *Codosiga hollandica* during degumming. iTRAQ data analysis showed Rds1, and pyruvate kinase I was decreased and increased in the kanef-degumming, respectively. Other DEPs of ferredoxin I, superoxide dismutase and aconitatehydratase were identified to be related to the Glyoxylate and dicarboxylate metabolism (ko00630).

Conclusions: Bacteria including *Chryseobacterium*, *Dysgonomonas*, *Acinetobacter*, *Lactococcus* and *Bacteroides*and fungi like *Wallemia hederae* and *Codosiga hollandica* are key candidate microbes for kanef degumming.

Keywords: Bio-degumming, *Hibiscus cannabinus*, Microbial diversity, iTRAQ

Background

Kenaf (*Hibiscus cannabinus*),which contains 8–16% lignin, 53–66% cellulose, 23–35% pectin and some hemicellulose, is an annual herbaceous bast fiber crop of the genus Malvaceae [1–3]. It is widely planted around the world, especially in the tropical and subtropical regions, such as Asia and Latin America. Kenaf fiber is widely used as an important basic raw material in textile, manufacturing and composite fabrication due to its strong pulling force [1, 4]. However, the retting methods can influence the quality of kenaf fiber.

Retting based on the intervention of bacteria and microbia enzymes promotes the development of the textile industry via resulting in a better quality of fibers. Conventional methods for the degumming of kenaf bast included traditional natural fermentation (water retting) and chemical degumming. In comparison with the

natural fermentation and chemical degumming, biological (bacterial and enzymatic) degumming presents a series of advantages including high efficiency, low pollution, low cost and high fiber quality [3, 5–7]. The secretion of bacteria promote the decomposition of material, which can be used for bacteria to continue to grow [6, 8]. Ideal bacterial strains for kenaf degumming should have the advantages of secreting pectinase, hemicellulose, and ligninase, but not cellulase [6–8].

The screening of superior bacterial strains with the activity of pectate lyase, pectinase, hemicellulase and/or ligninase and the preservation of the natural fiber structure and mechanical properties is crucial for biological degumming [7–9]. A series of bacterial strains have been identified with strong ability of retting or degumming, like *Bacillus cereus* hn1–1 [10], *B. pumilus* [7], *B. licheniformis* and *B. subtilis* [11] and *B. tequilensis* SV11-UV37 [6]. Cheng et al. [10] showed that the 10 h-degumming process by *B. cereus* hn1–1 produced a residual gum rate as low as 5% and the

* Correspondence: hunandsw@163.com
Institute of Bast Fiber Crops, Chinese Academy of Agriculture Sciences, Changsha 410000, China

fiber rate as high as 76%. Mao et al. [12] reported that the ramie retting could be completed within 56 h by using a microbia consortium RAMCD407 plus 0.2% NaOH, with 2.84% residual gum content and 5.2 cN/dtex breaking strength of the final fiber. In addition, our previous study [7] identified that pectinase and mannanase were the key enzymes in the degumming of kenaf bast mediated by bacteria including *B. pumilus, B. alcalophilus, Clostridium tertium, Brevibacillus brevis, Pectobacterium carotovora, Erwinia chrysanthemi,* and *Tyromyces subcaesius.* All these results suggested the pivotal roles of bacteria in the degumming of kenaf bast. However, there was no systematic analysis for the alterations of bacterial secretome during degumming of kenaf bast.

This study was performed to identify the key candidate microbes and secretory proteins during the retting and degumming of kenaf bast. Alterations of microbial proteomics and community during retting and degumming of kenaf bast was detected using isobaric tags for relative and absolute quantitation (iTRAQ) and 16S/18S rRNA sequencing, respectively. These findings provide novel insights into the retting and degumming of kenaf bast.

Results
Degumming of kenaf bast and bacteria collection
The weight loss rate of kenaf bast was gradually increased with degumming, ranging from 11.72% at 40 h and 32.06% at 190 h (Table 1). The bacterial viable count, however, was primarily decreased from initial 4.2×10^7 CFU/ml to 8.7×10^6 CFU/ml at 40 h post fermentation. It was increased to the maximum 5.1×10^8 CFU/ml at 150 h, followed with a decrease. These results might suggest that the growth of bacteria had degumming function.

General characteristics of 16S/18S rRNA sequencing
We then collected liquid samples at 0, 40, 110 and 150 h post retting and subjected to 16S/18S rRNA sequencing. A total of 167,321 and 181,887 raw reads was generated from 16S and 18S rRNA sequencing data, respectively. After removing the low-quality reads and chimera, the sequence length of trimmed reads is mostly distributed at 420 bp - 490 bp in bacteria, and the fungus sample is mostly distributed at 399 bp - 409 bp. The final rank abundance curve tends to a plateau, indicating that the sample species are richer in composition and higher in uniformity (Fig. 1). The higher species rank value of samples at 0 h (500–600) compared with of samples at
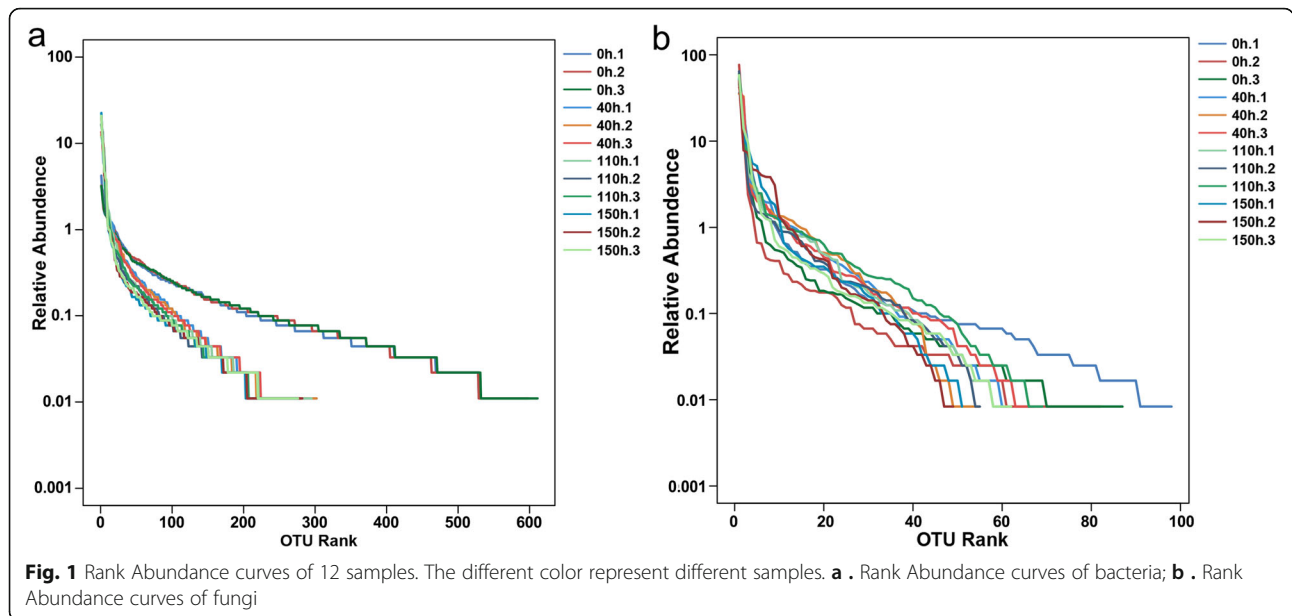
40, 110 and 140 h (200–300) indicated that the fermentation significantly decreased bacterial diversity. In addition, we found the retting significantly reduced the bacterial alpha diversity estimators like Chao 1, PD_whole_tree, Shannon and Simpson index (Table 2). In addition, retting also decreased fungal alpha diversity estimators including Chao 1 and PD_whole_tree, but increased Goods coverage (Table 2). These changes suggested retting decreased microbes viable count and bacterial diversity but increased fungal diversity.

Identification of key bacteria responsible for the degumming of kenaf bast
After OTUs (operational taxonomic units) annotation, we identified the abundances (at phylum level) of *Bacteroidetes* (from 34.91% at 0 h to 67.75% at 150 h) and *Patescibacteria* (1.00 to 9.53%) were gradually increased during the degumming of kenaf bast (Additional file 1: Figure S1), which replaced the *Proteobacteria*. The initial abundance of *Firmicutes* (2.83%) was firstly increased to 15.28% at 40 h and then decreased to 3.40% at 150 h (Additional file 1: Figure S1a and b). At the family level, *Sphingobacteriaceae* (10.98%, *Bacteroidetes*), *Flavobacteriaceae* (9.62%), *Burkholderiaceae* (8.13%), and *Sphingomonadaceae* (6.77%) were the dominant bacteria at the initial (Fig. 2a and b). However, they were replaced by the fast-growing [Weeksellaceae] (21.55%, *Bacteroidetes*), *Enterobacteriaceae* (16.41%, *Proteobacteria*) and *Moraxellaceae* (12.13%, *Proteobacteria*) families at 40 h post retting. The latter bacteria were gradually replaced by the *Bacteroidaceae* family from 40 h to 150 h (25.89%; Fig. 2a and b). We also identified that the growth of *Cytophagaceae* and *Chitinophagaceae* families (*Bacteroidetes*) were inhibited by retting process. Similar changes were found in several bacterial genera. Dominant genera, including *Pedobacter* (9.10%), *Flavobacterium* (6.86%), *Pseudomonas* (5.97%) and *Brevundimonas* (5.64%) kept an equivalent level at the initial (0 h). *Chryseobacterium* (15.03%, [Weeksellaceae]), *Acinetobacter* (12.10%, *Moraxellaceae*) and *Lactococcus* (8.84%, *Streptococcaceae* family) grew to be the dominant bacteria at 40 h, which were then replaced by *Bacteroides* (25.89%) in the fermentation liquid, followed by *Chryseobacterium* (16.03%) and *Dysgonomonas* families (15.96%) (Fig. 2c and d). These changes in bacterial abundances were in response to that of the bacterial viable count in Table 1. These data showed that *Acinetobacter, Chryseobacterium, Lactococcus* and *Bacteroidetes* at genus level and [Weeksellaceae], *Enterobacteriaceae, Moraxellaceae* and *Bacteroidaceae* at family level

Table 1 Kenaf bast degumming effect during different enrichment time

Terms	0 h	40 h	110 h	150 h	190 h
Weight loss rate (%)	–	11.72	24.45	31.26	32.06
Initial content of live bacterial (CFU/mL)	4.2×10^7	8.7×10^6	7.2×10^7	5.1×10^8	3.1×10^8

Fig. 1 Rank Abundance curves of 12 samples. The different color represent different samples. **a** . Rank Abundance curves of bacteria; **b** . Rank Abundance curves of fungi

might be key candidate bacteria responsible for the degumming of kenaf bast.

Identification of key fungi responsible for the degumming of kenaf bast

As expected, fungal abundances were also changed in response to degumming. All fungi were mainly dominated by 2 phyla: *Opisthokonta* (98.73%) and *SAR* (1.24%). The relative abundance of *Opisthokonta* subkingdom was gradually decreased to 85.09%, and replaced by *SAR* phylum (14.61% at 150 h; Fig. 3a). The dominant fungal families *Incertae Sedis* (61.11 to 8.10%) and *Pezizomycotina* (18.73 to 3.89%) were replaced by *Dipodascaceae* (5.98 to 53.08%) and some other fungi such as *Bulleribasidiaceae*, *Craspedida*, *Chrysophyceae*, etc. (Fig. 3b). At genus level, the results showed that *Wallemia* (60.43%) and *Eurotiomycetes* (18.55%) were the dominant fungi (Fig. 3c). As for

specific species, the dominant positions of *Wallemia hederae* (60.33%) at the initial, but decreased at 40 h (36.97%), 110 h (12.12%) and 150 h (7.50%) (Fig. 3d). The relative abundance of *Codosiga hollandica* species was increased from 0.16% at 0 h to 2.42% at 150 h.
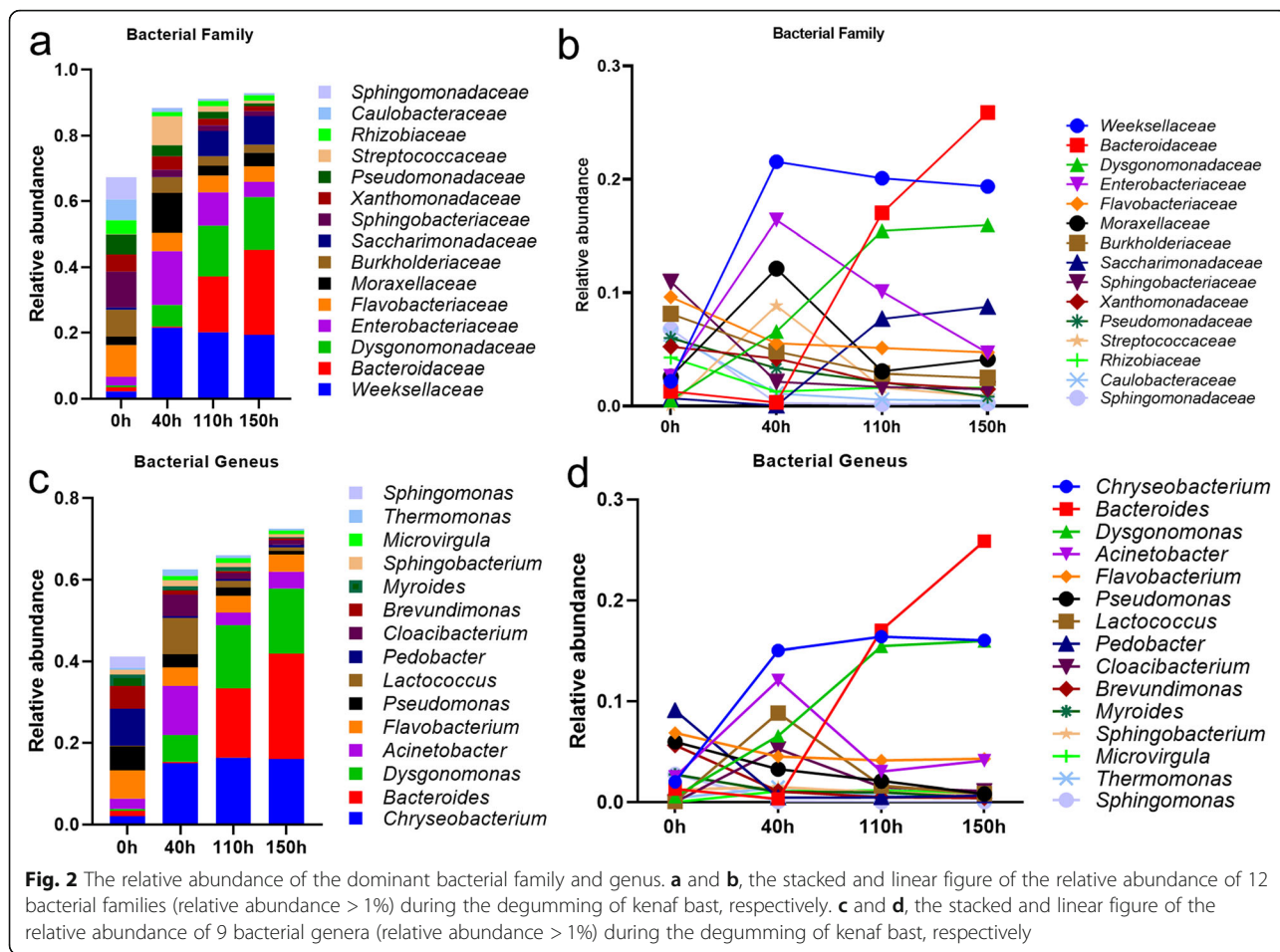
Microbia secretomics analysis and identification of candidate proteins or peptides

We then performed the secretomics analysis to identify the candidate proteins which might be responsible for biological degumming of kenaf bast, since there are significant changes in the relative abundance of bacteria and fungi. A total of 197 proteins, including 67 DEPs were identified (Additional file 2: Table S1). Clustering analysis showed the distinct expression patterns of these proteins in the samples (Fig. 4). We identified the significantly down regulated Rds1 protein peptides (including

Table 2 The alpha diversity of the 16S and 18S rRNA-seq

Group	16S rRNA-seq				
	Chao 1	Goods coverage	PD_whole_tree	Shannon	Simpson
0 h	642.47 ± 8.45 [a]	0.9920 ± 0.0002 [a]	25.62 ± 0.21 [a]	8.01 ± 0.05 [a]	0.9924 ± 0.0006 [a]
40 h	388.16 ± 13.70 [b]	0.9912 ± 0.0003 [b]	12.83 ± 0.14 [b]	5.53 ± 0.06 [b]	0.9447 ± 0.0015 [b]
110 h	341.90 ± 12.46 [c]	0.9923 ± 0.0003 [a]	11.52 ± 0.43 [c]	5.09 ± 0.17 [c]	0.9275 ± 0.0102 [c]
150 h	353.47 ± 5.32 [c]	0.9919 ± 0.0003 [a]	12.25 ± 0.19 [b]	4.75 ± 0.06 [d]	0.9058 ± 0.0043 [d]
	18S rRNA-seq				
0 h	98.86 ± 4.15 [a]	0.9988 ± 0.0004 [b]	3.09 ± 0.30 [a]	2.26 ± 0.59 [b]	0.58 ± 0.14 [b]
40 h	62.75 ± 3.77 [b]	0.9996 ± 0.0001 [a]	2.27 ± 0.32 [bc]	3.01 ± 0.07 [a]	0.75 ± 0.01 [a]
110 h	65.79 ± 3.94 [b]	0.9996 ± 0.0000 [a]	2.45 ± 0.23 [b]	2.75 ± 0.30 [ab]	0.64 ± 0.05 [ab]
150 h	56.10 ± 8.06 [b]	0.9997 ± 0.0002 [a]	1.92 ± 0.07 [cd]	2.78 ± 0.24 [ab]	0.69 ± 0.04 [ab]

Difference in one-way ANOVA is presented by different letters

Fig. 2 The relative abundance of the dominant bacterial family and genus. **a** and **b**, the stacked and linear figure of the relative abundance of 12 bacterial families (relative abundance > 1%) during the degumming of kenaf bast, respectively. **c** and **d**, the stacked and linear figure of the relative abundance of 9 bacterial genera (relative abundance > 1%) during the degumming of kenaf bast, respectively
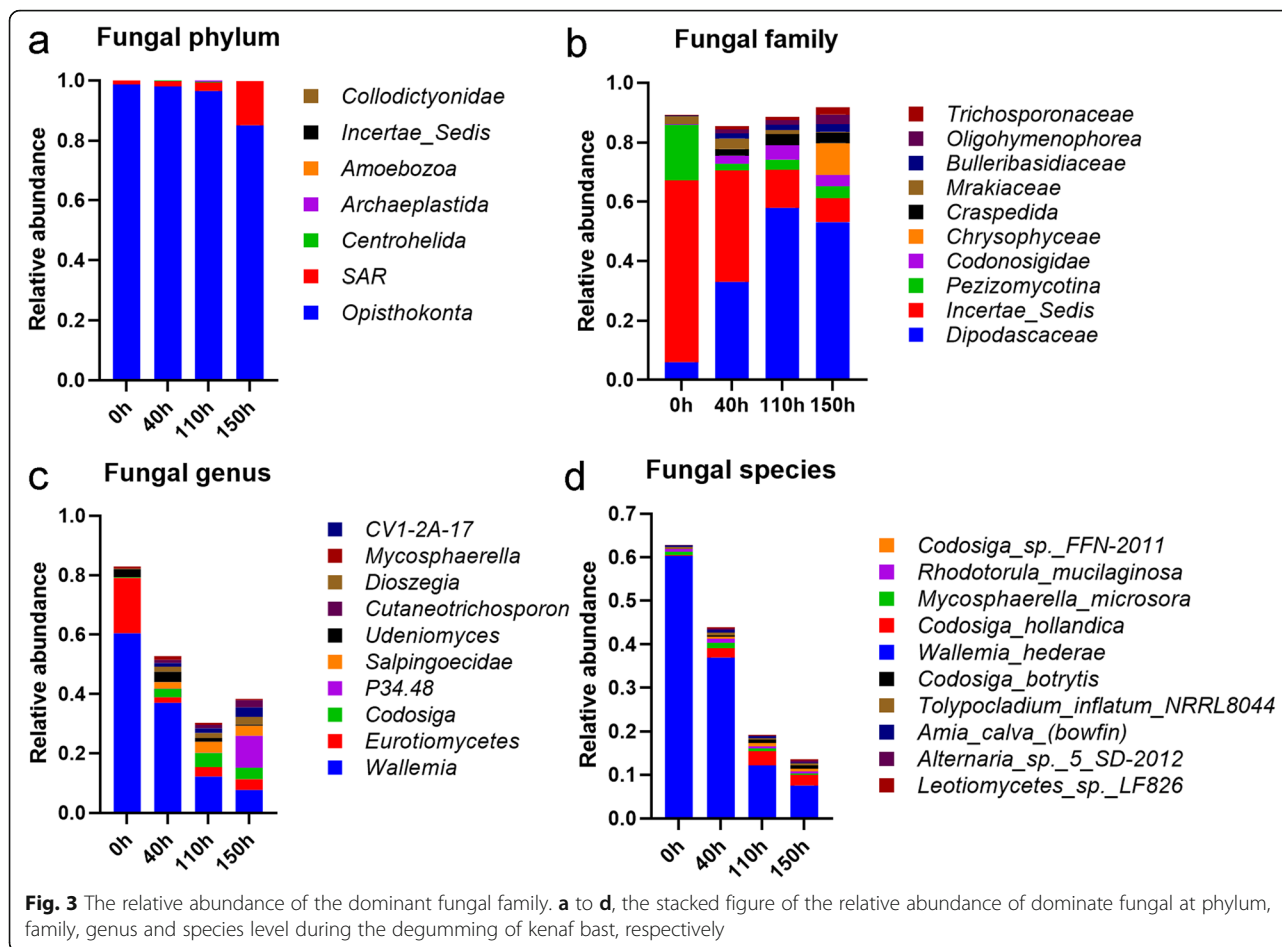
I4YCX5 and R9AEW5, A1DDU4, A0A0S7E3J2, A0A0J5 SQP1, Q4WVL1, B0Y1F6, A0A084BN00 and A0A0K8L4 F0), superoxide dismutase peptides (J1ACL6 and A0A0Q 9DZS2), and the upregulated peptides of pyruvate kinase I (A0A0A2W3C3), lipoprotein (A0A0N7K9K4), ferredoxin I (I4JHJ0), thioredoxin (A0A088F1E4, A0A0M2 Y158 and A0A0M3C9P8). A0A0A2W3C3 was enriched into the pathways including glucagon signaling pathway (ko04922) and pyruvate metabolism (ko0492). A peptide of aconitatehydratase (aconitase, ACO), which is related to the glyoxylate and dicarboxylate metabolism (ko0063 0), was decreased at 40 h and then increased at 110 and 150 h post retting compared with 0 h (Table 3). Most of the other peptides were annotated with transporter activities (Additional file 2: Table S1).

Among the other non-DEPs, we identified that the peptide of Aldehyde dehydrogenase family protein (A0A160 F3I4), Aspartate aminotransferase (A0A0A2VU16) and 6-phosphogluconate dehydrogenase (L8X2A2). The L8X2A2 was identified to be related with pentose phosphate pathway.

Discussion

The degumming of kenaf bast is a process mediated by dynamic change of microbes. Using the 16S/18S rRNA sequencing, we identified the changed bacterial and fungal abundance during the degumming of kenaf bast (0~ 150 h). In the fermentation liquid, the growth of *Cytophagaceae* and *Chitinophagaceae* was inhibited during the degumming of kenaf bast. Many bacteria genera played crucial roles in in the degumming process of kenaf bast, such as *Bacteroides, Chryseobacterium, Dysgonomonas, Acinetobacter,* and *Lactococcus,* of which the abundance were greatly changed with degumming treatment. Similarly, some fungi also participated in the degumming process of kenaf bast including *Pezizomycotina, Dipodascaceae, Codosiga hollandica,* and *Incertae Sedis.* The abundance of subdivided *Wallemia* and *Eurotiomycetes* genera were dramatically reduced in the process of dealkylation and fermentation. And the increased *Dipodascaceae* family might promote the degumming of kenaf bast. A series of *Bacillus* strains has been identified to be ramie- or kanef-degumming strains, like *B. cereus* hn1−1 [10], *B. pumilus*

Fig. 3 The relative abundance of the dominant fungal family. **a** to **d**, the stacked figure of the relative abundance of dominate fungal at phylum, family, genus and species level during the degumming of kenaf bast, respectively

[7], *B. licheniformis* and *B. subtilis* [11] and *B. tequilensis* SV11-UV37 [6]. In addition, our previous study [7] showed that seven bacterial strains belonging to the species including *B. pumilus*, *B. alcalophilus*, *C. tertium*, *Brevibacillus brevis*, *Pectobacterium carotovora*, *Erwinia chrysanthemi* and *Tyromyces* sub *caesius* were the key in strains for the degumming of kenaf bast. Other reports also showed the ability of *B. licheniformis*, *Paenibacillus macerans*, *C. tertium*, *B. tequilensis* and *B. vulgatus*or the proteases and pectinolytic enzymes derived from these strains for degumming fiber, wool and wood [6, 7, 13, 14]. For instance, enzymatic treatment is an acceptable method of intervention among the methods for wool treatment for breaking down the surface structure [14]. Serine proteases are the most common commercial proteases derived from *Bacillus* strains.

For the degumming of plant fibers, some researchers had isolated proteases, xylanases and pectate lyases from the bacteria like *Acinetobacter spp.* (> 1 species of the genus) [15] and *B. cereus* [16] and fungi including Extremophilic fungi [17–19]. Researchers also identified the lignin degrading role of *Pseudomonas*, *Lactococcus* and *Acinetobacter* strains in hemp, ramie and mechanical pulp

[20–23]. For instance, Hu et al. [23] observed that abundances of *Pseudomonas* and *Acinetobacter* were increased to the highest at 36 h post retting and decreased subsequently. In particular, the finding about *Acinetobacter* and *Lactococcus* was consistent with our results, which was increased to 12.09 and8.84% at 40 h and then decreased to 4.10 and 0.84% at 150 h. The dynamic changes of these bacteria during the degumming of kanef bast suggested their crucial roles in degrading kanef.

Kanef-degumming is a dynamic process of bacterial adaptation and growth. The initial stage is characterized by decreased bacterial richness and diversity [24]. We determined the decreased bacterial viable count at the 40 h post retting, followed by increased bacterial viable count but not bacterial richness and diversity. Our present study presented a cluster of anaerobic *Bacteroidaceae* members like *Bacteroides*, *Chryseobacterium* and *Dysgonomonas*, played crucial roles in the degumming of kanef bast, especially in the late stage. *Cytophagaceae* was initially inhibited, which might guarantee the fiber structure. The rapid growth of anaerobic *Bacteroidaceae* bacteria changed bacterial diversity. Xylan and pentose (including xylose) are main components of hemicellulose in plants [25]. The degradation of hemicellulose into
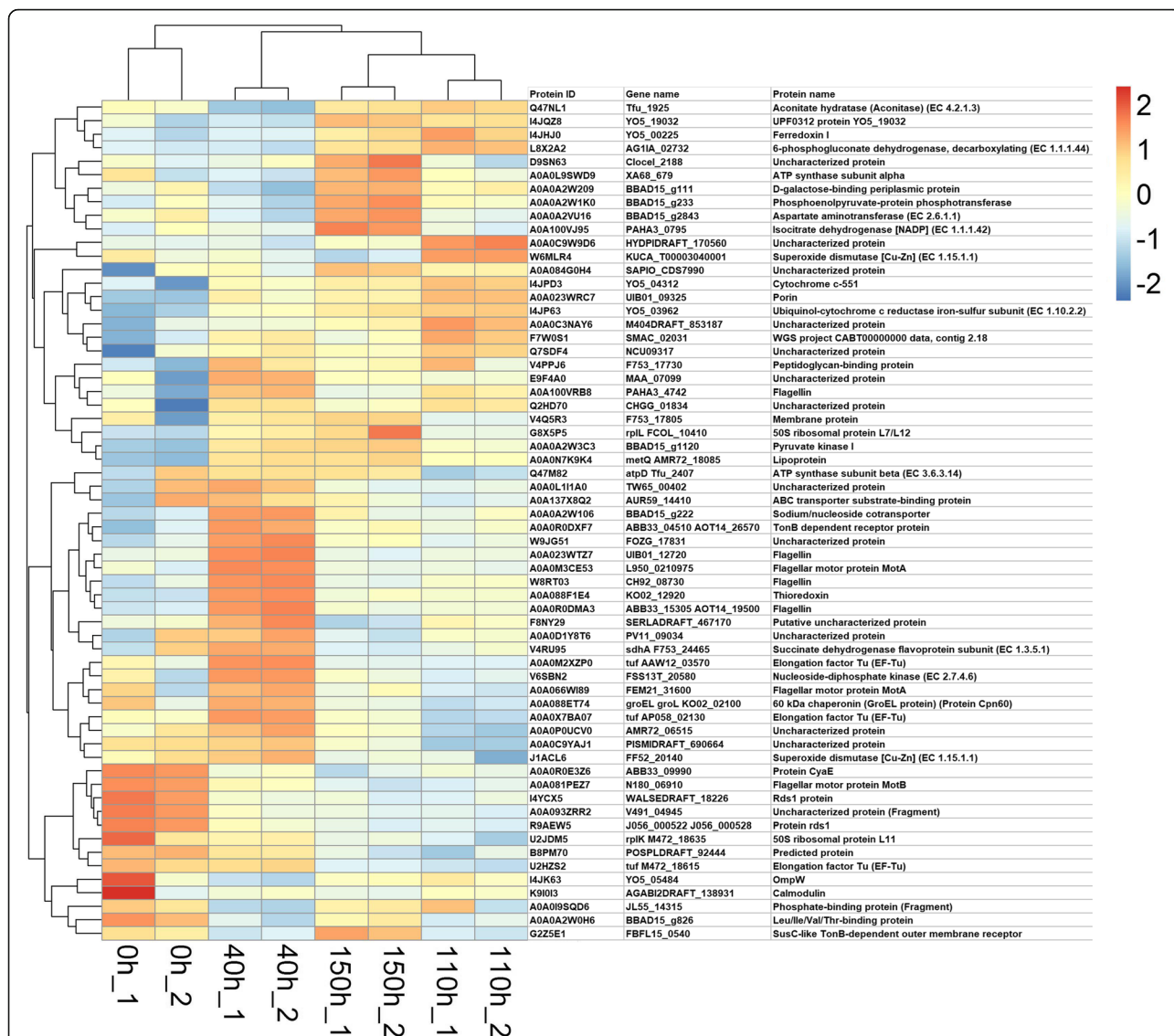
Protein ID	Gene name	Protein name
Q47NL1	Tfu_1925	Aconitate hydratase (Aconitase) (EC 4.2.1.3)
I4JQZ8	YO5_19032	UPF0312 protein YO5_19032
I4JHJ0	YO5_00225	Ferredoxin I
L8X2A2	AG1IA_02732	6-phosphogluconate dehydrogenase, decarboxylating (EC 1.1.1.44)
D9SN63	Clocel_2188	Uncharacterized protein
A0A0L9SWD9	XA68_679	ATP synthase subunit alpha
A0A0A2W209	BBAD15_g111	D-galactose-binding periplasmic protein
A0A0A2W1K0	BBAD15_g233	Phosphoenolpyruvate-protein phosphotransferase
A0A0A2VU16	BBAD15_g2843	Aspartate aminotransferase (EC 2.6.1.1)
A0A100VJ95	PAHA3_0795	Isocitrate dehydrogenase [NADP] (EC 1.1.1.42)
A0A0C9W9D6	HYDPIDRAFT_170560	Uncharacterized protein
W6MLR4	KUCA_T00003040001	Superoxide dismutase [Cu-Zn] (EC 1.15.1.1)
A0A084G0H4	SAPIO_CDS7990	Uncharacterized protein
I4JPD3	YO5_04312	Cytochrome c-551
A0A023WRC7	UIB01_09325	Porin
I4JP63	YO5_03962	Ubiquinol-cytochrome c reductase iron-sulfur subunit (EC 1.10.2.2)
A0A0C3NAY6	M404DRAFT_853187	Uncharacterized protein
F7W0S1	SMAC_02031	WGS project CABT00000000 data, contig 2.18
Q7SDF4	NCU09317	Uncharacterized protein
V4PPJ6	F753_17730	Peptidoglycan-binding protein
E9F4A0	MAA_07099	Uncharacterized protein
A0A100VRB8	PAHA3_4742	Flagellin
Q2HD70	CHGG_01834	Uncharacterized protein
V4Q5R3	F753_17805	Membrane protein
G8X5P5	rplL FCOL_10410	50S ribosomal protein L7/L12
A0A0A2W3C3	BBAD15_g1120	Pyruvate kinase I
A0A0N7K9K4	metQ AMR72_18085	Lipoprotein
Q47M82	atpD Tfu_2407	ATP synthase subunit beta (EC 3.6.3.14)
A0A0L1I1A0	TW65_00402	Uncharacterized protein
A0A137X8Q2	AUR59_14410	ABC transporter substrate-binding protein
A0A0A2W106	BBAD15_g222	Sodium/nucleoside cotransporter
A0A0R0DXF7	ABB33_04510 AOT14_26570	TonB dependent receptor protein
W9JG51	FOZG_17831	Uncharacterized protein
A0A023WTZ7	UIB01_12720	Flagellin
A0A0M3CE53	L950_0210975	Flagellar motor protein MotA
W8RT03	CH92_08730	Flagellin
A0A088F1E4	KO02_12920	Thioredoxin
A0A0R0DMA3	ABB33_15305 AOT14_19500	Flagellin
F8NY29	SERLADRAFT_467170	Putative uncharacterized protein
A0A0D1Y8T6	PV11_09034	Uncharacterized protein
V4RU95	sdhA F753_24465	Succinate dehydrogenase flavoprotein subunit (EC 1.3.5.1)
A0A0M2XZP0	tuf AAW12_03570	Elongation factor Tu (EF-Tu)
V6SBN2	FSS13T_20580	Nucleoside-diphosphate kinase (EC 2.7.4.6)
A0A066WI89	FEM21_31600	Flagellar motor protein MotA
A0A088ET74	groEL groL KO02_02100	60 kDa chaperonin (GroEL protein) (Protein Cpn60)
A0A0X7BA07	tuf AP058_02130	Elongation factor Tu (EF-Tu)
A0A0P0UCV0	AMR72_06515	Uncharacterized protein
A0A0C9YAJ1	PISMIDRAFT_690664	Uncharacterized protein
J1ACL6	FF52_20140	Superoxide dismutase [Cu-Zn] (EC 1.15.1.1)
A0A0R0E3Z6	ABB33_09990	Protein CyaE
A0A081PEZ7	N180_06910	Flagellar motor protein MotB
I4YCX5	WALSEDRAFT_18226	Rds1 protein
A0A093ZRR2	V491_04945	Uncharacterized protein (Fragment)
R9AEW5	J056_000522 J056_000528	Protein rds1
U2JDM5	rplK M472_18635	50S ribosomal protein L11
B8PM70	POSPLDRAFT_92444	Predicted protein
U2HZS2	tuf M472_18615	Elongation factor Tu (EF-Tu)
I4JK63	YO5_05484	OmpW
K9I0I3	AGABI2DRAFT_138931	Calmodulin
A0A0I9SQD6	JL55_14315	Phosphate-binding protein (Fragment)
A0A0A2W0H6	BBAD15_g826	Leu/Ile/Val/Thr-binding protein
G2Z5E1	FBFL15_0540	SusC-like TonB-dependent outer membrane receptor

Columns: 0h_1, 0h_2, 40h_1, 40h_2, 150h_1, 150h_2, 110h_1, 110h_2

Fig. 4 The heatmap of the 64 differentially expressed proteins/peptides. Red and blue represents the high and low expression, respectively. _1 and 2 represent biological repeat 1 and 2 in each group, respectively

oligomers and sugarsis a metabolic property shared by sugar-fermenting *Bacteroides* [26–29]. The increased abundance of these *Bacteroidaceae* members might suggest the accumulation of their substrates derived from the early stage fermentation from aerobic bacteria like *Acinetobacter* and *Lactococcus* or the changed environments.

In addition, we also identified the down regulation of several peptides of Rds1 during the degumming of kanef bast. Rds1 a stress-responsible protein, which could be depressed by starving from glucose, ammonium, phosphate, exposuring to carbon dioxide and high temperature [30]. The down regulation of it was theoretically in line with the hypothesis that the starvation of sugar and oxygen of early retting stage. What's more, the identification of the gradually decreased halophilic *Wallemia hederae* and increased turfgrass

pathogen in the fermentation liquid might suggest the deterioration of fermentation. *Codosiga hollandica.*

Conclusions

In conclusion, we identified a cluster of key bacteria responsible for the degumming of kanef bast. We identified that the growth of *Cytophagaceae* was initially inhibited at the early stage of degumming for kenaf bast. The up-and-down change in the abundance of *Acinetobacter* and *Lactococcus* (*Streptococcaceae*) and the gradually increased growth of *Bacteroides*, *Chryseobacterium*, *Dysgonomonas* characterized the degumming process. In addition, we also identified the increased *Codosiga hollandica* and decreased *Wallemia hederae* fungus family during degumming for 150 h. Secretory proteomics analysis showed Rds1, pyruvate

Table 3 Several differentially expressed proteins in during degumming

Protein ID	Time (s)				Protein name	Gene ontology	Pathway
	0 h	40 h	110 h	150 h			
R9AEW5;A1DDU4; A0A0S7E3J2; A0A0J5SQP1; Q4WVL1;B0Y1F6; A0A084BN00; A0A0K8L4F0	4391.5	715.0	340.8	362.7	Protein rds1		
A0A0N7K9K4	889.5	2642.3	1897.0	2776.1	Lipoprotein		
A0A023WRC7	308.7	614.1	981.2	671.3	Porin	integral component of membrane [GO:0016021]; porin activity [GO:0015288]	
I4YCX5	15, 628.3	386.7	228.8	254.1	Rds1 protein		
A0A0A2W3C3	964.2	4595.7	2396.7	5424.1	Pyruvate kinase I		ko04922: Glucagon signaling pathway; ko0492: Pyruvate metabolism
I4JHJ0	580.1	651.8	2090.5	1518.2	Ferredoxin I		
Q47NL1	816.8	199.8	2134.1	1615.2	Aconitate hydratase (Aconitase) (EC 4.2.1.3)	4 iron, 4 sulfur cluster binding [GO:0051539]; aconitate hydratase activity [GO:0003994]; metabolic process [GO:0008152]	ko00630: Glyoxylate and dicarboxylate metabolism
A0A088F1E4; A0A0M2Y158; A0A0M3C9P8	201.3	1957.3	429.8	1047.9	Thioredoxin	protein disulfide oxidoreductase activity [GO:0015035]; cell redox homeostasis [GO:0045454]; glycerol ether metabolic process [GO:0006662]	
J1ACL6; A0A0Q9DZS2	393.9	447.6	286.3	325.2	Superoxide dismutase [Cu-Zn] (EC 1.15.1.1)	metal ion binding [GO:0046872]; superoxide dismutase activity [GO:0004784]	
W6MLR4;W0TF05; A0A090C5A2	1289.9	1014.2	2316.6	770.7	Superoxide dismutase [Cu-Zn] (EC 1.15.1.1)	metal ion binding [GO:0046872]; superoxide dismutase activity [GO:0004784]	
V4RU95;S6LCD6; M2UZN0;L0GJW1; I4JML0;I4CTX4; H7F0P7;F8H871; F2MXE8;A4VKP6; A0A137Y7T1; A0A137WWW6; A0A0I9SRB2; A0A0H3YZE1; A0A0D7EA74; A0A0C2MWX1; A0A098FQU9; A0A061JVN2; A0A023WTY8	1525.4	2439.2	1244.5	1037.6	Succinate dehydrogenase flavoprotein subunit (EC 1.3.5.1)	plasma membrane [GO:0005886]; flavin adenine dinucleotide binding [GO:0050660]; succinate dehydrogenase (ubiquinone) activity [GO:0008177]; electron transport chain [GO:0022900]; tricarboxylic acid cycle [GO:0006099]	
A0A0D1Y8T6	1129.9	1915.8	958.2	658.1	Uncharacterized protein	succinate dehydrogenase activity [GO:0000104]	
H7FVF4	147.3	38.6	124.9	289.2	Isocitrate lyase (EC 4.1.3.1)	isocitrate lyase activity [GO:0004451]; carboxylic acid metabolic process [GO:0019752]	

kinase I and aconitatehydratase peptides were changed during the degumming of kanef bast. These findings provide evidence on the crucial roles of these microbes in the degumming of kenaf bast.

Methods
Bacteria collection and degumming of kenaf bast
Humus samples (50 g) were collected from Sanya, China. Water samples (100 ml) were collected from a conventional retting pond (50 cm away from the water surface) in Xiaoshan, Zhejiang, China. Soil samples (50 g) were collected from continuous cropping soil of Kenaf in Xiaoshan. Soil and humus samples were diluted into 100 ml bacteria free water (autoclave at 121 °C for 20 min), filtered and then mixed with the above water samples.

Kenaf bast was collected from Xianghongma No. 1 plants in Changsha, China. The samples were cut into pieces (3 cm) and then immersed into bacteria mixture (10 g: 5 ml) with supplementation of 100 ml bacteria free water. For the degumming of kenaf bast, samples were

maintained on an orbital shaker at 30 °C, pH 7.0, for 30 min. Then the fermentation liquid samples were collected at 0, 40, 110, 150 and 190 h post degumming and used for further analysis. Each experiment was done in triplicates.

Determination of kenaf bast weight loss rate and viable count of bacteria

The weight loss rate of the kenaf bast samples in each condition was calculated according to the following formula: weight loss rate (%) = [initial weight (10 g)-final weight (g) of kenaf bast]/initial weight (10 g) of kenaf bast × 100%. Total viable count was quantified traditionally using the colony-forming units (CFUs) after incubation on nutrient broth solid media (pH 7.0) for 0–190 h.

DNA extraction and 16S and 18S ribosomal RNA gene sequencing

DNA extraction was performed using a PowerSoil™ DNA Isolation Kit (MOBIO laboratories, San Diego, Carlsbad, California, USA). The concentration and purity of the DNA was measured by agarose gel electrophoresis. The 16S ribosomal DNA (rDNA) gene V3-V4 region of the bacteria was amplified by PCR with bar coded primers (343F: 5′- TAC GGRAGGCAGCAG – 3′ and 798R: 5′- AGGGTATCTA ATCCT-3′), using FastPfu Polymerase (TransStart, Beijing, China). The PCR primers for the 18S rDNA of fungus were NS1: 5′- GTAGTCATATGCTTGTCTC – 3′ and NS8: 5′- TCCGCAGGTTCACCTACGGA – 3′. Reaction parameters were: 95 °C for 5 min, followed by 30 cycles of 95 °C 30 s, 52 °C 45 s (16S) or 1 min (18S), 72 °C 1 min, and the final step of 72 °C for 10 min. The amplicons of 16S and 18S rDNA were purified by an AxyPrep DNA Gel Extraction Kit (Axygen Biosciences, Union City, California, USA). After repeating the above steps (amplification and purification), the concentration of final purified amplicons was detected by Qubit 2.0 (Thermo Fisher Scientific, Walthan, Massachusetts, USA). At the end, the samples were pooled and subjected to an Illumina MiSeq Instrument (Illumina, San Diego, California, USA) in Shanghai OE Biotech. Co., Ltd. with 350 bp paired-end sequencing.

Data processing

Raw data from different samples were identified based on the unique barcode. The primer sequences were removed and data were trimmed using U-Search software [31]. FLASH v1.2.7 software (http://ccb.jhu.edu/software/FLASH) was used for merging paired-end reads and the counting of reads [32]. The chimeric sequences were removed using UCHIME (http://www.drive5.com/usearch/index.html) [33]. Sequences were clustered into OTUs by QIIME (v1.8.0, http://qiime.org/) [34] according to the minimal 97% similarity. Through matching to the Silva database (https://www.arb-silva.de/) [35], the

taxonomic information for each OTU was obtained. Alpha and beta diversities were analyzed to determine differences among groups in terms of species complexity by QIIME (v1.8.0) software.

Protein extraction, digestion, and iTRAQ labeling

Fermentation liquid samples (30 ml) were collected at 0 h, 40 h, 110 h and 150 h, and then centrifuged at 1500 g for 10 min in an Eppendorf centrifuge (Eppendorf, San Diego, California, USA). The supernatants were collected and filtered through a 0.22 μm membrane. Samples were then diluted into precooled TCA/acetone (1:9) solutions (1: 4 v/v) and then stored at – 20 °C overnight. Pellets were collected by centrifugation (Sigma Aldrich, Schnelldorf, Germany) at 17000 g for 30 min, followed by washing with precooled acetone (90%) for three times. The precipitate was air-dried and then dissolved in sodium dodecyl sulfonate lysate supplementing (Beyotime, Shanghai, China) with protease inhibitor cocktail (P8340, Sigma, USA) on a homogenizer (Hai Shu Ke Sheng, Ningbo, Zhejiang, China). The crude precipitates were collected by centrifugation at 12000 g for 10 min at 4 °C (Sigma Aldrich, Schnelldorf, Germany). The supernatant was selected after sonication by centrifugation (12,000 g for 15 min) for twice. Finally, the supernatant was stored at – 80 °C for further use. The concentration of protein was measured using BCA method [36], with BCA Protein Assay Kit (Thermo Scientific Dionex, San Jose, USA). The integrity of the extracted protein was detected by SDS-PAGE [37].

The quantified samples were then digested according to the filter aided sample preparation procedure as previously described [38]. In brief, 100 μg of protein was precipitated by precooled acetone (1:5 v/v) at – 20 °C for 1 h, centrifuged at 16000 g for 10 min at 4 °C, and vacuum freeze-dried. Protein precipitation was prepared using an iTRAQ kit (Applied Biosystems, Carlsbad, California, USA) following the manufacturer's instructions. The marked samples were then mixed, dried and then subjected to separation and identification.

2D-LC-MS/MS analysis

The freeze-dried sample was dissolved in 110 μL of the mobile phase A solution. Peptide separation was performed on an Agilent 1200 HPLC (Agilent Technologies, Foster City, California, USA) with the Narrow-Bore column (2.1 mm × 150 mm × 5 μm), analytical guard column (4.6 × 12.5 mm, 5-Micron), flow rate of 0.3 ml/min, at 210 nm and 280 nm in Shanghai Luming Biotech. Co., Ltd. Reverse phase chromatographic analyses were performed using Nano-RPLC Buffer A (Applied Biosystems), PepMap100C18 column (75 μm × 20 mm, 3 μm, NanoViper; Thermo Scientific Dionex, San Jose, USA) with the mobile phase B increased from 5 to 35% in 70 min. The Q Exactive Orbitrap mass spectrometer (Thermo Fisher Scientific, Bremen, Germany;

Duan *et al. BMC Genomics*　　(2020) 21:121

Page 9 of 10

nano-electrospray ionization, 1.6 kV, 250 °C) was used for data-dependent acquisition according to the previously reported method [39].

Protein identification and quantification

The raw proteomics data in the format of .raw was aligned to UniProt database (https://www.uniprot.org/) using Maxquant 1.5.1.0 (Version 1.5.1.0; Thermo Fisher Scientific). Proteins and peptides with fold discovery rate < 0.01 were retained as for further identification of differentially expressed peptides/proteins (DEPs). The significant different proteins between groups were identified with the threshold of T-test p value ≤0.05 and fold change (FC) ≥ 1.2.

Bioinformatics analysis

For annotation of the DEPs, Gene Ontology (GO, http://www.geneontology.org) and Kyoto Encyclopedia of Genes and Genomes (KEGG, http://www.genome.jp/kegg/) databases were used for the gene functions prediction. The GO classifications of molecular function, biological process and cellular component and the pathways significantly related to these DEPs were identified with the criteria of $p < 0.05$.

Statistical analysis

Data were expressed as the mean ± standard deviation. The SPSS 22.0 software was employed for the statistical analysis. One-way ANOVA test was performed to analyze the differences. Comparison of differences between groups was detected using t-test. The p-value < 0.05 was considered as significantly difference.

Supplementary information

Supplementary information accompanies this paper at https://doi.org/10.1186/s12864-020-6531-2.

Additional file 1 Figure S1. The relative abundance of the dominant bacterial phyla. a and b, the stacked and linear figure of the relative abundance of 8 phyla during the degumming of kenaf bast, respectively.

Additional file 2 Table S1. The list of the differentially expressed proteins/peptides in the degumming of the kenaf bast.

Abbreviations

ACO: Aconitase; CFUs: Colony-forming units; DEPs: Differentially expressed proteins/peptides; FC: Fold change; GO: Gene Ontology; iTRAQ: Isobaric tag for relative and absolute quantitation; KEGG: Kyoto Encyclopedia of Genes and Genomes; OTUs: Operational taxonomic units (OTUs); rDNA: Ribosomal DNA

Authors' contributions
DSW summarized the sequencing data, performed the data analysis and prepared the original manuscript. DSW and CLF attended discussion and revised MS. FXY attended data re-interpreting discussion. DSW, CLF, FXY, YQ, LZY and ZK prepared the plant material and attended the transcriptomes data analyses and discussion. DSW and PYD designed the experiments, provided research platform, performed the pathway enrichment analysis, and revised the manuscript. All authors approved the final manuscript.

Availability of data and materials
The original data were uploaded to SRA database (https://www.ncbi.nlm.nih.gov/sra) and the BioProject ID is PRJNA562024.

Ethics approval and consent to participate
Not applicable.

Consent for publication
Not applicable.

Competing interests
The authors declare that they have no competing interests.

References

1. Ramesh M. Kenaf (*Hibiscus cannabinus L.*) fibre based bio-materials: A review on processing and properties. Prog Mater Sci. 2016;78:1–92.
2. Ayadi R, Hanana M, Mzid R, Hamrouni L, Khouja M, Salhi HA. *Hibiscus cannabinus L.*–kenaf: a review paper. J Nat Fibers. 2017;14:466–84.
3. Ververis C, Christodoulakis N, Santas R, Santas P, Georghiou K. Effects of municipal sludge and treated waste water on biomass yield and fiber properties of kenaf (*Hibiscus cannabinus L.*). Ind Crop Prod. 2016;84:7–12.
4. Zaleha M, Mahzan S, Fitri M, Kamarudin K, Eliza Y, Tobi AM. Wave velocity characteristic for Kenaf natural fibre under impact damage. IOP Conf. Ser. Mater Sci Eng. 2017;165:012018.
5. Zhao D, Pan C, Ping W, Ge J. Degumming crude enzyme produced by *Bacillus cereus* HDYM-02 and its application in flax retting. BioResources. 2018;13:5213–24.
6. Chiliveri SR, Koti S, Linga VR. Retting and degumming of natural fibers by pectinolytic enzymes produced from *Bacillus tequilensis* SV11-UV37 using solid state fermentation. SpringerPlus. 2016;5:1–17. https://doi.org/10.1186/s40064-016-2173-x.
7. Duan S, Cheng L, Liu Z, Feng X, Zheng K, Peng Y. Diversity and characteristics of Kenaf Bast degumming microbial resources. J Nat Fibers. 2018;15:799–807.
8. Saha M, Rana RS, Adhikary B, Mitra S. Screening of bacterial strains for pectate lyase production and detection of optimal growth conditions for enhanced enzyme activity. J Appl Nat Sci. 2017;9:370–4.
9. Ramesh D, Ayre BG, Webber CL, D'Souza NA. Dynamic mechanical analysis, surface chemistry and morphology of alkali and enzymatic retted kenaf fibers. Text Res J. 2015;85:2059–70.
10. Cheng L, Wang Q, Feng X, Duan S, Yang Q, Zheng K, Liu Z, Liu Z, Peng Y. Screening a bacterium and its effect on the biological degumming of ramie and kenaf. Sci Agr. 2018;75:375–80.
11. Donaghy JA, Levett PN, Haylock RW. Changes in microbia populations during anaerobic flax retting. J Appl Microbiol. 2010;69:634–41.
12. Mao K, Chen H, Qi H, Qiu Z, Zhang L, Zhou J. Visual degumming process of ramie fiber using a microbia consortium RAMCD407. Cellulose. 2019;26:3513–28.
13. Shinde S. Significance of microbiological tests in technical textiles. Man-Made Textiles in India. 2010;53:241–9.
14. McDevitt JP, Winkler J: Method for enzymatic treatment of wool. In: Google Patents; 2000.
15. Salwan R, Sharma V, Pal M, Kasana RC, Yadav SK, Gulati A. Heterologous expression and structure-function relationship of low-temperature and alkaline active protease from *Acinetobacter* sp. IHB B 5011 (MN12). Int J Biol Macromol. 2018;107:567–74.
16. Kohli P, Gupta R. Application of calcium alginate immobilized and crude pectin lyase from *Bacillus cereus* in degumming of plant fibres. Biocatal Biotransfor. 2019;37:341–8.

17. Salwan R, Sharma V. Proteases from Extremophilic Fungi: a tool for white biotechnology: 3rd ISNPS. France: Avignon; 2016.

18. Gundala PB, Chinthala P. Extremophilic pectinases. In: *Extremophilic Enzymatic Processing of Lignocellulosic Feedstocks to Bioenergy*: Springer; 2017. p. 155–80. https://link.springer.xilesou.top/chapter/10.1007/978-3-319-54684-1_9#citeas.

19. Polizeli M, Rizzatti A, Monti R, Terenzi H, Jorge JA, Amorim D. Xylanases from fungi: properties and industrial applications. Appl Microbiol Biot. 2005;67:577–91.

20. Tuomela M, Hatakka A, Raiskila S, Vikman M, Itävaara M. Biodegradation of radiolabelled synthetic lignin (14 C-DHP) and mechanical pulp in a compost environment. Appl Microbiol Biot. 2021;55:492–9.

21. Ribeiro A, Pochart P, Day A, Mennuni S, Bono P, Baret J-L, Spadoni J-L, Mangin I. Microbia diversity observed during hemp retting. Appl Microbiol Biot. 2015;99:4471–84.

22. Wang Q. Chen H-g, fang G, Chen A-q, Yuan P, Liu J-s. isolation of *Bacillus cereus* P05 and *Pseudomonas* sp. X12 and their application in the ramie retting. Ind Crop Prod. 2017;97:518–24.

23. Hu Q, Zhang J, Xu C, Li C, Liu S. The dynamic microbiota profile during pepper (*Piper nigrum L.*) peeling by solid-state fermentation. Curr Microbiol. 2017;74:739–46.

24. Zhao D, Liu P, Pan C, Du R, Ping W, Ge J. Bacterial succession and metabolite changes during flax (*Linum usitatissimum L.*) retting with *Bacillus cereus* HDYM-02. Sci Rep. 2016;6:31812.

25. Saha BC. Hemicellulose bioconversion. J ind microbiol biot. 2003;30:279–91.

26. Matte A, Forsberg CW, Gibbins AMV. Enzymes associated with metabolism of xylose and other pentoses by *Prevotella (Bacteroides) ruminicola* strains, *Selenomonas ruminantium* D, and *Fibrobacter succinogenes* S85. Can J Microbiol. 1992;38:370–6.

27. Van Maris AJ, Winkler AA, Kuyper M, De Laat WT, Van Dijken JP, Pronk JT. Development of efficient xylose fermentation in *Saccharomyces cerevisiae*: xylose isomerase as a key component: *Biofuels*. Springer; 2007. p. 179–204. https://link.springer.xilesou.top/chapter/10.1007/10_2007_057.

28. Moysés D, Reis V, Almeida J, Moraes L, Torres F. Xylose fermentation by *Saccharomyces cerevisiae*: challenges and prospects. Int J Mol Sci. 2016;17:207.

29. Solden LM, Hoyt DW, Collins WB, Plank JE, Daly RA, Hildebrand E, Beavers TJ, Wolfe R, Nicora CD, Purvine SO. New roles in hemicellulosic sugar fermentation for the uncultivated Bacteroidetes family BS11. ISME J. 2017;11:691.

30. Ludin KM, Hilti N, Schweingruber ME. *Schizosaccharomyces pombe rds1*, an adenine-repressible gene regulated by glucose, ammonium, phosphate, carbon dioxide and temperature. Mol Gen Genet. 1995;248:439–45.

31. Edgar RC. Search and clustering orders of magnitude faster than BLAST. Bioinformatics. 2010;26:2460–1.

32. Deepak R, Shengdar QT, Cyd K, Jennifer AF, Jeffry DS, Keith J. FLASH assembly of TALENs for high-throughput genome editing. Nat Biotechnol. 2012;30:460–5.

33. Edgar RC, Haas BJ, Clemente JC, Christopher Q, Rob K. UCHIME improves sensitivity and speed of chimera detection. Bioinformatics. 2011;27:2194–200.

34. Caporaso JG, Kuczynski J, Stombaugh J, Bittinger K, Bushman FD, Costello EK, Fierer N, Peña AG, Goodrich JK, Gordon JI, Huttley GA, Kelley ST, Knights D, Koenig JE, Ley RE, Lozupone CA, McDonald D, Muegge BD, Pirrung M, Reeder J, Sevinsky JR, Turnbaugh PJ, Walters WA, Widmann J, Yatsunenko T, Zaneveld J, Knight R. QIIME allows analysis of high-throughput community sequencing data. Bioinformatics. 2010;7:335–6.

35. Quast C, Pruesse E, Yilmaz P, Gerken J, Schweer T, Yarza P, Peplies J, Glöckner FO. The SILVA ribosomal RNA gene database project: improved data processing and web-based tools. Nucleic Acid Res. 2012;41:D590–6.

36. Smith PK, Krohn Rl, Hermanson GT, Mallia AK, Gartner FH, Provenzano MD, Fujimoto EK, Goeke NM, Olson BJ, Klenk DC. Measurement of protein using bicinchoninic acid. Anal Biochem. 1985;150:76–85.

37. Giovanni C, Maurizio B, Luca M, Laura S, Gian Marco G, Barbara C, Paola O, Luciano Z, Pier GR. Blue silver: a very sensitive colloidal Coomassie G-250 staining for proteome analysis. Electrophoresis. 2010;25:1327–33.

38. Wisniewski J, Zougman A, Nagaraj N, Mann M. Universal sample preparation method for proteome analysis. Nat Methods. 2009;6:359–62.

39. Yu H, Wang X, Xu J, Ma Y, Zhang S, Yu D, Fei D, Muhammad A. iTRAQ-based quantitative proteomics analysis of molecular mechanisms associated with Bombyx mori (Lepidoptera) larval midgut response to BmNPV in susceptible and near-isogenic strains. J Proteome. 2017;165:S1874391917302105.

Publisher's Note